Mudslides during Hurricane Ivan and an Assessment of the Potential for Future Mudslides in the Gulf of Mexico

by

Mary C. Nodine, Stephen G. Wright, and Robert B. Gilbert, The University of Texas at Austin, and E.G. Ward, Offshore Technology Research Center

Phase I Project Report
Prepared for the Minerals Management Service
Under the MMS/OTRC Cooperative Research Agreement
1435-01-04-CA-35515
Task Order 39239
MMS Project Number 552

October 2006

OTRC Library Number: 10/06C175

"The views and conclusions contained in this document are those of the authors and should not be interpreted as representing the opinions or policies of the U.S. Government. Mention of trade names or commercial products does not constitute their endorsement by the U. S. Government".

For more information contact:

Offshore Technology Research Center
Texas A&M University
1200 Mariner Drive
College Station, Texas 77845-3400
(979) 845-6000

or

Offshore Technology Research Center
The University of Texas at Austin
1 University Station C3700
Austin, Texas 78712-0318
(512) 471-6989

A National Science Foundation Graduated Engineering Research Center

TABLE OF CONTENTS

TABLE OF CONTENTS i

LIST OF TABLES AND FIGURES ii

INTRODUCTION iii

Objective iii
Publications iii
Background iv
Scope v

MUDSLIDE DAMAGE IN THE MISSISSIPPI DELTA REGION OF THE GULF OF MEXICO 1

ANALYTICAL MODEL 2

Limit Equilibrium Model Spreadsheet Program 3

SHEAR STRENGTH DATA 4

MUDSLIDE SUSCEPTIBILITY ANALYSES 5

Regional Analysis 5

Site-Specific Analyses 7

Mississippi Canyon Block 20 Analysis 12

STABILITY CHART FOR THE LIMIT EQUILIBRIUM MODEL 15

CONCLUSION 19

References 20

APPENDIX A - EQUATIONS IN THE LIMIT EQUILIBRIUM MODEL 22

APPENDIX B – SHEAR STRENGTH PROFILES FROM PUBLIC SOURCES 25

APPENDIX C - USER'S GUIDE FOR THE LIMIT EQUILIBRIUM SPREADSHEET PROGRAM 29

LIST OF TABLES AND FIGURES

Table 1. Sample factor of safety calculations using chart for linear increase in strength. 17

Figure 1. Locations of pipelines damaged by mudslides during Hurricane Ivan and inferred mudslide locations superimposed on map of mudslide prone areas from Coleman et al.2 1
Figure 2. Locations of borings from which shear strength data were obtained 4
Figure 3. Factor of safety ranges at mudslide locations, based on selected shear strength profiles 6
Figure 4. Factor of safety contours assuming an undrained shear strength of 50 psf at the surface, increasing linearly with depth at the rate of 8 psf/ft 7
Figure 5. Calculated factors of safety at shear strength data points 8
Figure 6. Site-specific analyses where pipelines were damaged (Boring location at South Pass 49 is approximate.) 9
Figure 7. Site-specific analyses where pipelines were not damaged 10
Figure 8. Overview of site-specific shear strength data points, illustrating the variability in factor of safety within lease blocks and between various geologic features 11
Figure 9. Effect of slope angle on factor of safety for Mississippi Canyon Block 20 13
Figure 10. Effect of wave period on factor of safety at various water depths for Mississippi Canyon Block 20 14
Figure 11. Chart to calculate factor of safety against mudslide initiation for a strength profile increasing linearly with depth. 16
Figure 12. Shear strength profiles and corresponding linear strength profiles for example sites 17
Figure A1. Geometry of the limit equilibrium model 22
Figure C1. Model geometry 30
Figure C2. User interface for the spreadsheet program 30
Figure C3. Locations of initial input values 31
Figure C4. Site parameters 32
Figure C5. Maximum pressure on the sea floor 32
Figure C6. Shear strength profile 32
Figure C7. Trial heights 33
Figure C8. Factor of safety calculated from initial input values 34
Figure C9. Minimum factor of safety within range of heights 34
Figure C10. Minimum factor of corresponding with minimum height 35
Figure C11. Critical circle height entered in to table to calculate circle properties 36
Figure 12. Radii and factors of safety for slip circles extending to each depth in the shear strength profile 36
Figure C13. Identification of properties of the critical slip circle 37

INTRODUCTION

Objective

The objective of this research was to examine and review the mudflow/mudslide areas in the Gulf of Mexico caused by Hurricane Ivan, and to use this information to develop and evaluate practical methods for quantifying mudslide hazard.

The tasks for Phase I as outlined in the project proposal are as follows.

> ***Task 1:*** Review existing data on seafloor movements, including pipeline movements and failures, during Hurricane Ivan to identify the locations where movements occurred and the extent of movements.
>
> ***Task 2:*** Review pre-Ivan soil data including data on soil properties (unit weights, undrained shear strength) for selected areas where large soil movements were observed or expected.
>
> ***Task 3:*** Select representative sites for analyses and further study based on the locations of movements and the available soil data. Also select and include a nearby site where the seafloor appeared to remain stable during Ivan.
>
> ***Task 4:*** Determine wave conditions during Ivan at the selected sites. Obtain Hurricane Ivan oceanographic data.
>
> ***Task 5:*** Analyze seafloor stability at the representative sites selected in Task 3 to predict the potential for instability and soil movements. Data assembled in Task 1, 2 and 4 will be used in these analyses.
>
> ***Task 6:*** Final Report on Phase 1.

Publications

Nodine, M.C., Wright, S.G., Gilbert, R.B., and Ward, E.G. (2006), "Mudflows and Mudslides During Hurricane Ivan," *Proc. Offshore Technology Conference*, Houston, Texas, OTC Paper No. 18328.

Background

Large hurricanes in the Gulf of Mexico can generate waves large enough to trigger submarine slope failures, commonly referred to as “mudslides”. This became particularly evident in 1969 when the large (at least 70 feet high) waves generated by hurricane Camille produced a mudslide in the South Pass Block 70 area of the Gulf of Mexico that destroyed one offshore oil platform and severely damaged at least one other (Sterling and Strobeck[1]). Following this mudslide, considerable attention was devoted by the offshore oil industry to developing numerical and analytical models that could be used to predict when mudslides might occur and for estimating movements as a basis for designing measures to mitigate damage due to such events.

Coleman et al.[2] examined sediment instabilities in the offshore Mississippi River Delta region of the Gulf of Mexico and identified a large area of instabilities and mudslide activity. This area of mudslide activity included South Pass Block 70 where the mudslide referred to above occurred. In general the area identified by Coleman et al has been considered a mudslide susceptible area and facilities in this area have generally required special attention in design.

The recent hurricane Ivan in 2004 resulted in large ocean waves that again are believed to have been responsible for triggering mudslides that damaged offshore facilities. Hurricane Ivan is of particular interest because the waves are believed to have been significantly higher than waves that have previously been known to cause mudslides. In addition, the periods of the waves are somewhat longer that those of waves in previous large hurricanes and this may also have aggravated the impact. The wave and mudslide events associated with Hurricane Ivan provide an excellent opportunity to reexamine the areas of the Gulf of Mexico that are expected to be susceptible to mudslides as well as to verify numerical models that have been developed to predict hurricane-induced mudslides.

Scope

This report presents results of the research for MMS Project 552 as outlined in Tasks 1-6, listed above. It includes locations of known mudslide damage caused by hurricane Ivan. It also includes descriptions of data used to analyze the mudslide hazard in the Mississippi Delta region of the Gulf of Mexico, including Hurricane Ivan wave hindcast data, bathymetric data, and soil shear strength data. A limit equilibrium method used to analyze the data is described and presented in two practical forms: a chart that can be used to find the factor of safety against mudslide initiation for a site where the undrained shear strength increases linearly with depth, and an Excel spreadsheet computer program that can be used to calculate the factor of safety for sites with more complicated shear strength profiles. A regional analysis of the data is presented, including ranges in factors of safety for the mudslide locations using all the available shear strength profiles in the Mississippi Delta region of the Gulf of Mexico. Site specific analyses are presented where site-specific shear strength data were available, and a parametric analysis is presented for a site in the Mississippi Canyon lease block 20.

MUDSLIDE DAMAGE IN THE MISSISSIPPI DELTA REGION OF THE GULF OF MEXICO

Pipelines damaged by mudslides during Hurricane Ivan and the general locations of mudslide activity are shown in Figure 1. Information on observed mudslide damage from the damage spreadsheets provided by MMS[3] and in the literature (Coyne et al.[4] and Thompson et al.[5]) was combined with pipeline location data found on the MMS website[6] in order to accurately determine the locations of mudslides. The areas of mudflow gullies, mudflow lobes, and slightly disturbed sea floor mapped by Coleman et al.[2] are also shown in the figure. Most of the damage attributed to mud slides occurred within the area of mudflow lobes delineated by Coleman et al.

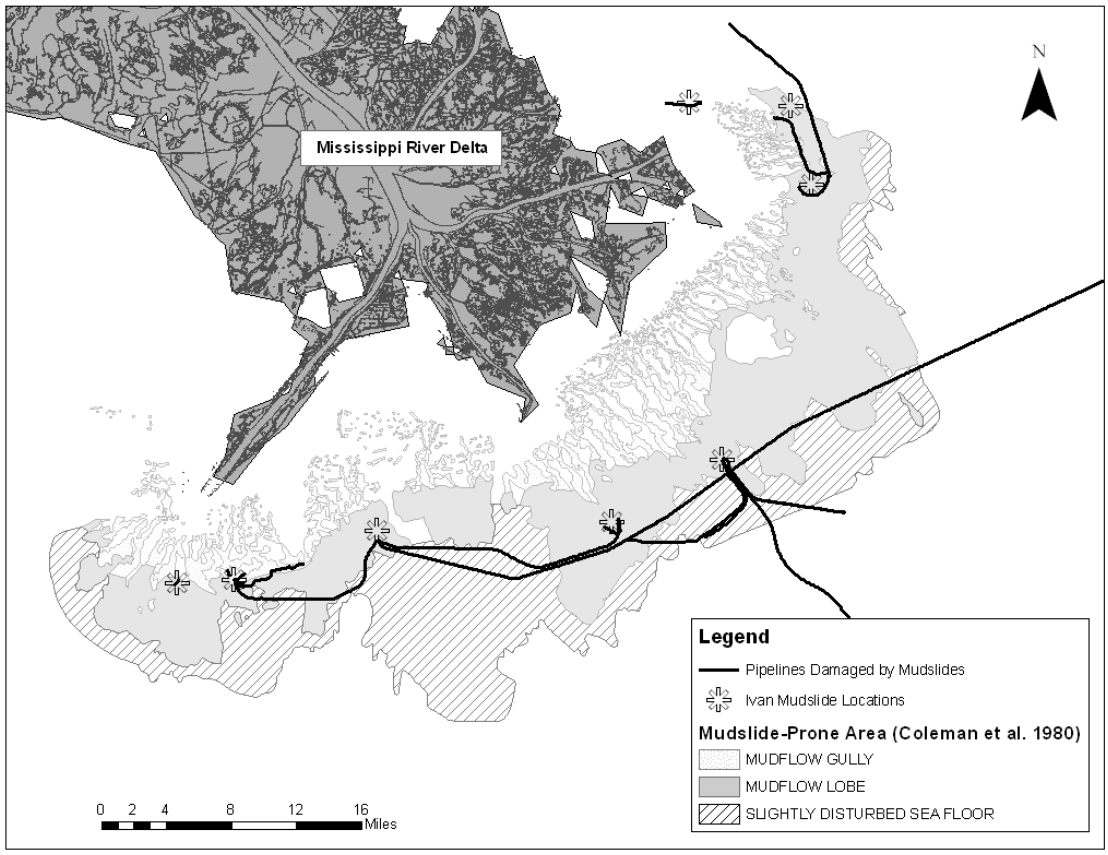

Figure 1. Locations of pipelines damaged by mudslides during Hurricane Ivan and inferred mudslide locations superimposed on map of mudslide prone areas from Coleman et al.2

ANALYTICAL MODEL

Shortly before and for a period of time after Hurricane Camille and the mudslide that damaged several offshore platforms in 1969, considerable attention was directed to developing numerical models that could be used to predict when mudslides might occur and the magnitude of soil movements associated with such events. The first such model was proposed by Henkel[7] based on the principles of limit equilibrium slope stability analysis. This was followed by the development of finite element models (Wright and Dunham[8], Wright[9]) as well as several layered continua models employing either visco-elastic or nonlinear hysteretic soil constitutive models (e.g. Schapery and Dunlap[10], Pabor[11]).

The various models used to calculate wave-induced soil movements and mudslides consider the wave on the ocean surface to produce a corresponding set of pressures at the sea floor. These pressures represent the change in pressure from the mean hydrostatic values and depend on the water depth, ocean wave height, and wave period (or wave length). Although some of the models developed to compute soil movements consider the stresses and displacements in the overlying water to be coupled with those of the subsurface soils, many simpler models consider the water and soil to be uncoupled and calculate the wave pressures assuming a rigid seafloor. This uncoupled approach was the approach used in the simple limit equilibrium model developed by Henkel[7]. In this model an equilibrium equation is written by summing moments about the center of a circular slip surface. The moments include driving moments due to the change in water pressure on the sea floor caused by the ocean wave and an additional driving moment produced by the weight of the soil and a sloping seafloor. The resisting moment is provided by shear stresses (τ) developed along the length of the circular slip surface. A factor of safety is defined as the ratio of the undrained shear strength of the soil to the developed shear stresses., i.e.

$$F = \frac{c}{\tau}$$

where “c” represents the undrained shear strength.

Henkel's limit equilibrium model was used for the analyses presented in this paper. The model has been found to provide a reasonable estimate of when instabilities are likely, i.e. the factor of safety is less than one, and without more extensive soil strength and stress-strain data for the areas of interest, use of more rigorous models is not warranted.

The equations used in the limit equilibrium model are presented in detail in Appendix 1.

Limit Equilibrium Model Spreadsheet Program

A spreadsheet program that can be used to analyze the mudslide susceptibility of a submarine site is included with this report as a Microsoft Excel file. The spreadsheet program calculates the factor of safety against mudslide initiation for any location with a piecewise linear shear strength profile. The spreadsheet calculates the minimum factor of safety for a site by calculating the factors of safety for various slip circles of different sizes (center point location and radius). A user's guide to accompany the spreadsheet program is attached in Appendix 3.

SHEAR STRENGTH DATA

Soil shear strength information for the Mississippi Delta region of the Gulf of Mexico was obtained from Bea et al.[12], Dunlap et al.[13], Hooper[14,15] and Roberts et al.[16], as well as from proprietary sources. Soil profiles obtained from public sources are attached in Appendix 2. Where shear strength data was not available to a depth of 150 feet or more, regional data on shear strength versus depth was obtained from a proprietary source in order to approximate the soil profiles up to a depth of 150 feet. This data is in the form of contour maps of shear strength at various depths in the Gulf of Mexico, created by a geotechnical consulting company for the purpose of offshore project planning. For context, a typical profile in the Gulf of Mexico for a normally consolidated clay has an undrained shear strength that increases at approximately 8 psf per foot (e.g., Quiros et al.[17]). In addition, a typical profile of undrained shear strength in the Gulf of Mexico for a remolded clay is generally at or above a profile that increases at 2 psf per foot (e.g., Quiros et al.[17]). These reference profiles are included on the profiles in Appendix 2 for comparison. Locations of all borings from which shear strength data were obtained are shown in Figure 2. Locations for some of the borings are approximate because some published reports did not include boring coordinates or detailed location maps.

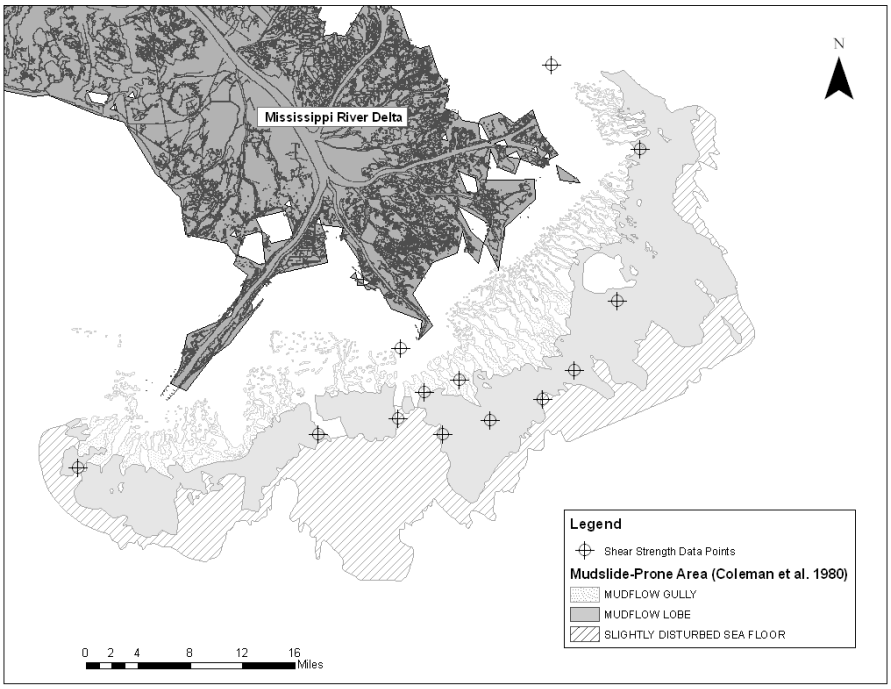

Figure 2. Locations of borings from which shear strength data were obtained

MUDSLIDE SUSCEPTIBILITY ANALYSES

Regional Analysis

The shear strength profiles used in this study cover a large area and vary greatly from location to location. Due to their wide variation, these profiles are believed to be representative of the range of undrained shear strengths in the delta. Because site-specific shear strength data were not available at all mudslide locations, factors of safety were calculated for each location of mudslide activity for the strongest and weakest of the available shear strength profiles for the region. These soil strength profiles are shown in Appendix 2. The strongest soil profile, representing the maximum factor of safety for each site, came from the boring in Mississippi Canyon 63. (The factor of safety calculated using the boring in South Pass 54 actually results in higher factor of safety, but Mississippi Canyon 63 was used because the profile for South Pass 54 was completed using regional data from shear strength contours.) The weakest soil profile, representing the minimum factor of safety for each site, came from a boring in South Pass 34 (the more linear of the two strength profiles available). Though these soil profiles consistently correspond with the maximum and minimum factors of safety in this study, this would not always be the case if wave heights and periods were significantly different than those that occurred during Hurricane Ivan.

The factors of safety calculated using the strongest and weakest soil profiles represent a range of possible factors of safety representing possible soil strengths. For each site, the wave loading is determined by the height and period of the wave of maximum height. The maximum wave height and the peak spectral period were taken from hindcast data for Hurricane Ivan[18], and the peak spectral period was taken as a reasonable approximation (i.e., within 10 percent) of the period of the maximum wave. The slope at each site is calculated from the bathymetry (Coleman et al.[2]).

The range in factors of safety computed using all of the available strength profiles is shown in Figure 3 for each of the locations of mudslide activity. The results were consistent with observed failures. The smallest factor of safety in each location was smaller than 1.0, indicating that a mudslide might be expected.

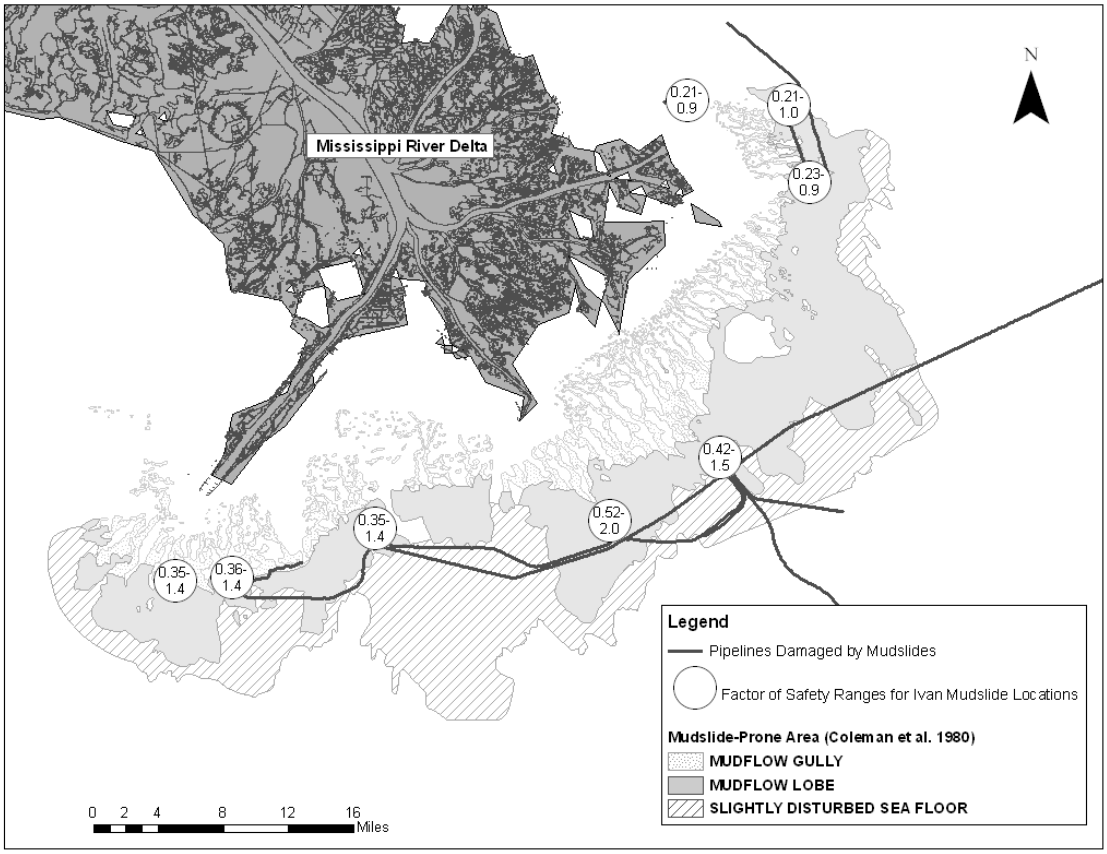

Figure 3. Factor of safety ranges at mudslide locations, based on selected shear strength profiles

Outside the range of very soft, underconsolidated clays in the mudslide-prone area, the undrained shear strength of the soil in the Gulf of Mexico is expected to increase with depth at a rate of at least 8 psf per foot (e.g., Quiros et al.[17]). Factors of safety were calculated for the area from the Mississippi Delta offshore region to the approximate location of the eye of Hurricane Ivan using the hindcast wave data and an undrained shear strength profile with a nominal value of 50 psf at the mudline and an increase of 8 psf per foot. Figure 4 shows contours of these factors of safety. There is no location outside the mudslide-prone area where the factor of safety is less than 1.0. This observation is consistent with the observations from Hurricane Ivan in that all of the reported mudslides are in the mudslide-prone area.

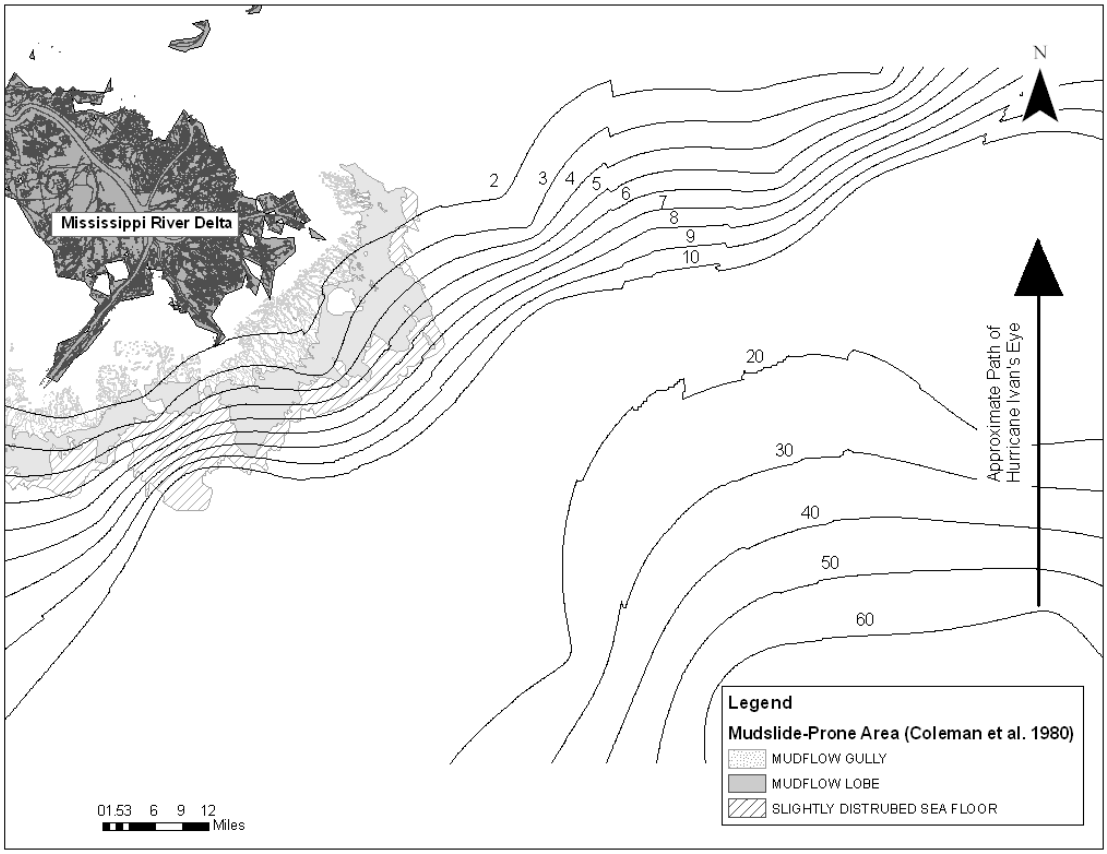

Figure 4. Factor of safety contours assuming an undrained shear strength of 50 psf at the surface, increasing linearly with depth at the rate of 8 psf/ft

Site-Specific Analyses

Factors of safety were calculated for each of the specific locations where shear strength data were available, using the wave hindcast and slope information as described in the previous section. The calculated factors of safety against mudslide initiation at each location where shear strength data are available are shown in Figure 5. In some locations, a range of safety factors is shown representing calculations for two or three shear strength profiles at the same location.

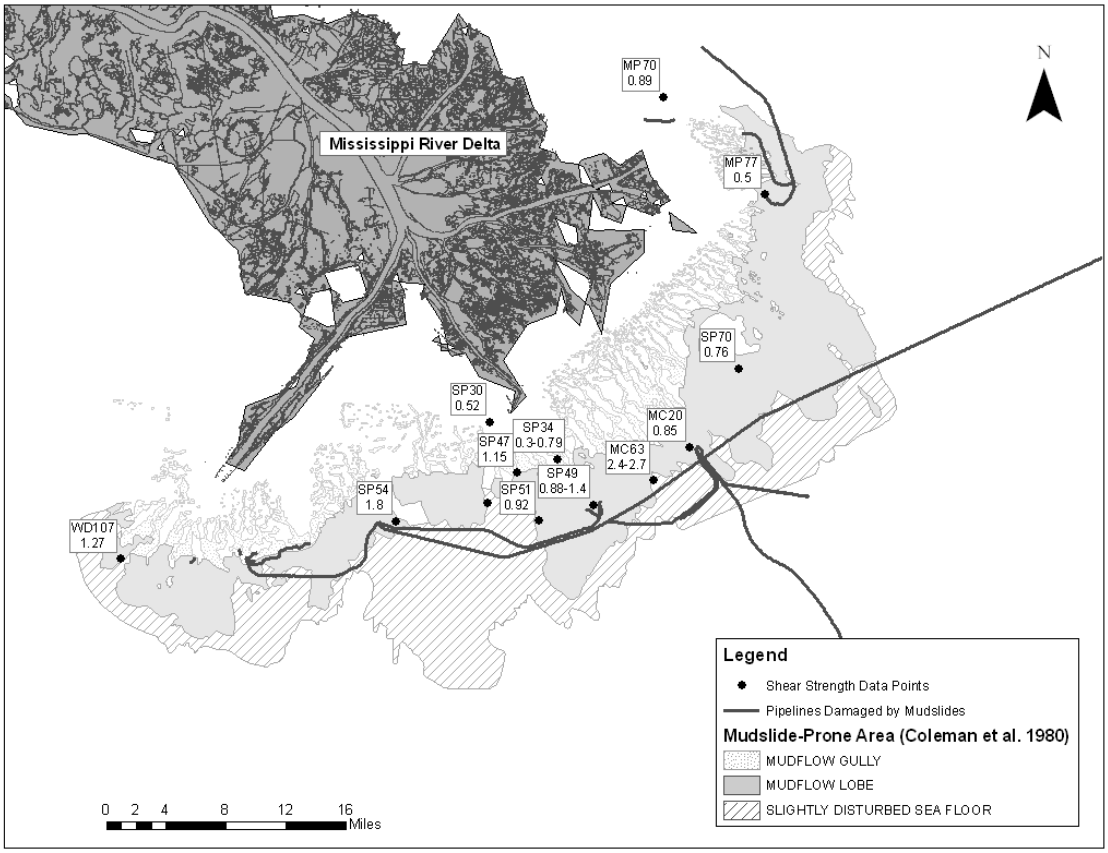

Figure 5. Calculated factors of safety at shear strength data points

Some of the sites where shear strength data were available are at or near the locations of pipelines, making them useful for site-specific analyses where mudslides were or were not known to occur. At lease blocks Mississippi Canyon 20 and Main Pass 77, mudslides were reported, and shear strength data were available near these sites. At Mississippi Canyon 20, the calculated factor of safety was 0.85, and at Main Pass 77 the calculated factor of safety was 0.50. At South Pass 49, a mudslide occurred, and analyses using three strength profiles near the site resulted in a range of factors of safety from 0.88-1.4. At all three of these sites where mudslides occurred, the minimum factor of safety was less than 1.0. Thus, the results suggest that the limit equilibrium model works well in these areas. However, the range in factors of safety at South Pass 49 illustrates the large variation in strength that may occur in the mud lobe area. Detailed plan views of the sites at Mississippi Canyon 20, Main Pass 77, and South Pass 49 are shown in Figure 6.

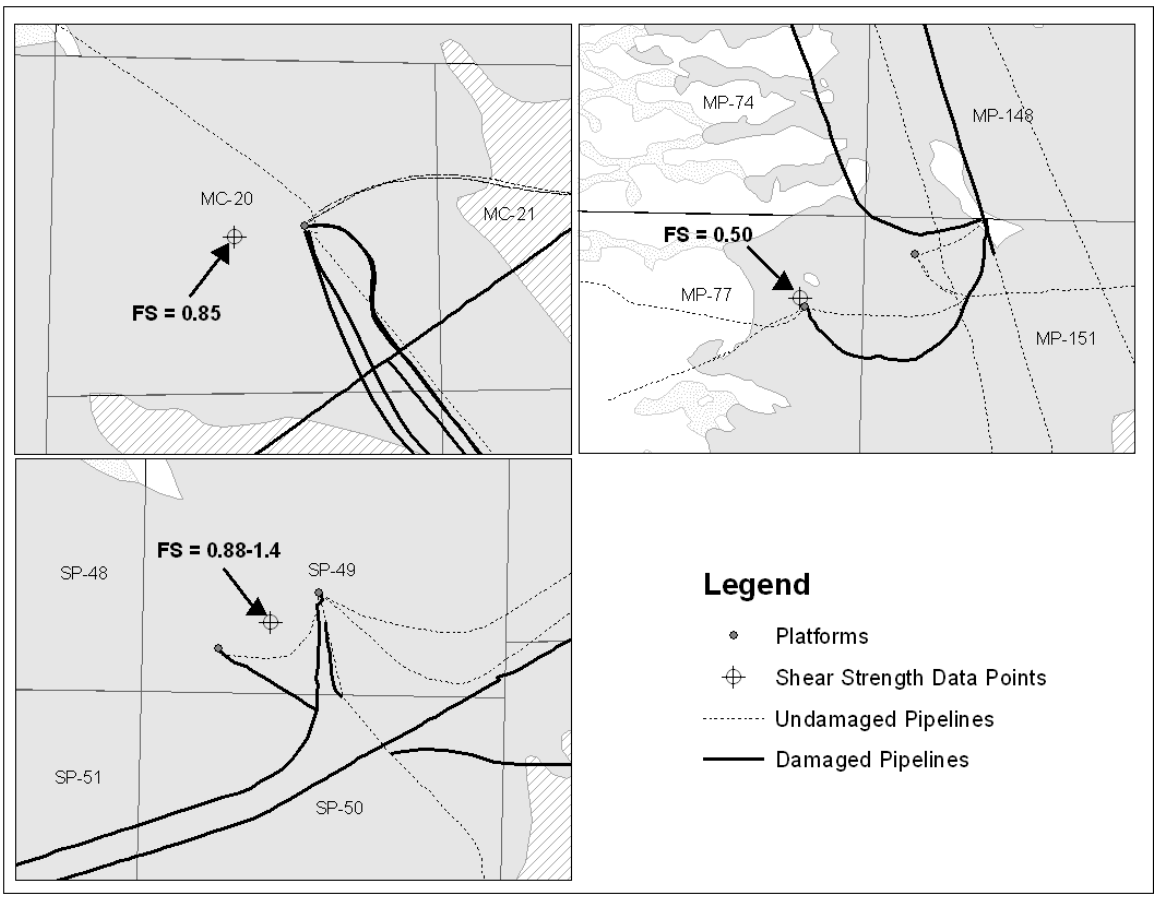

Figure 6. Site-specific analyses where pipelines were damaged (Boring location at South Pass 49 is approximate.)

At three locations within the mudslide-susceptible area delineated by Coleman et al.[2], site-specific shear strength data allowed validation of the model where platforms were not reportedly destroyed by mudslides. In South Pass 47, South Pass 54, and West Delta 107, shear strength profiles are available at the locations of platforms. The factors of safety calculated at these locations were 1.08, 1.76, and 1.27, respectively, and none of these platforms or the attached pipelines suffered damage during Hurricane Ivan. Detailed images of these three sites are shown in Figure 7.

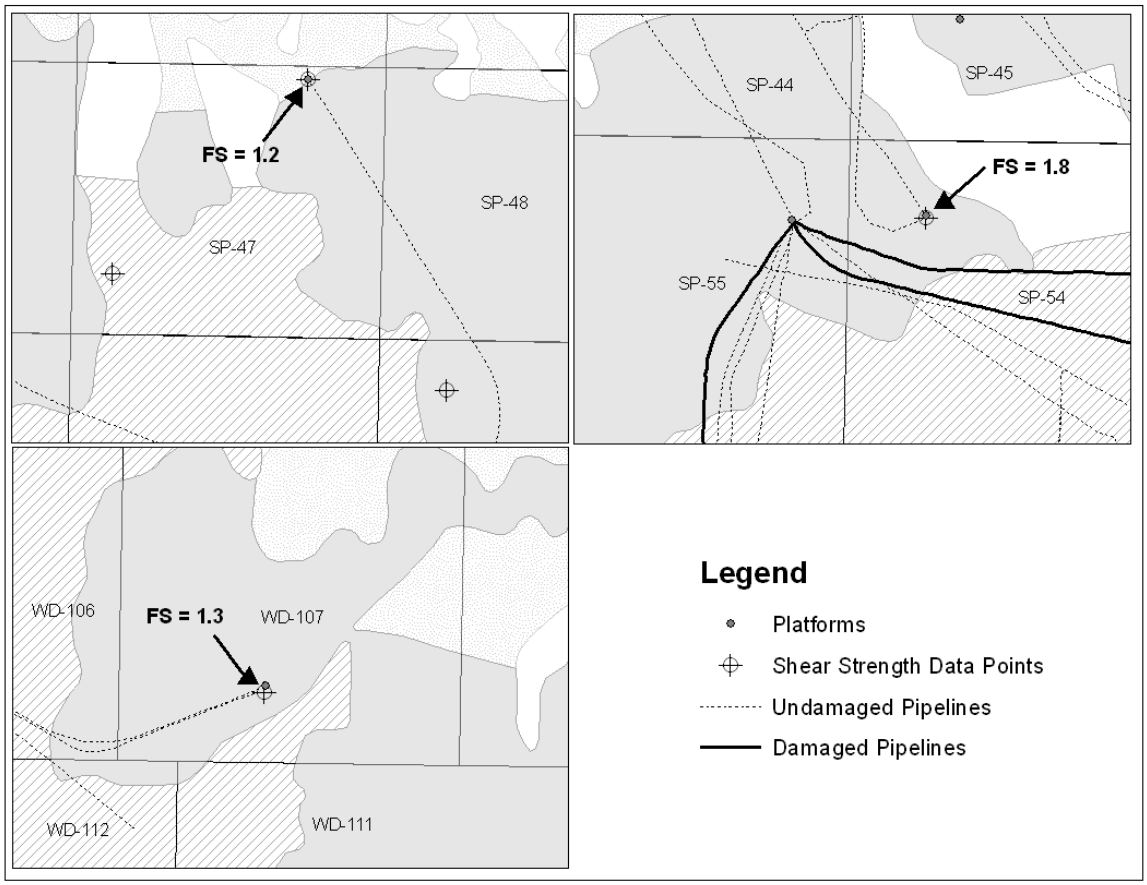

Figure 7. Site-specific analyses where pipelines were not damaged

An overview of the area encompassing many of the locations shown in Figure 6 and 7 is shown in Figure 8. The factors of safety calculated at points where shear strength data are available are listed on the figure. The values illustrate the large variability in factor of safety within a relatively small region. The soil shear strengths, and therefore the factors of safety, are highly dependent on the mudflow lobe and gully features in this region. The scale of these features in some locations is smaller than one lease block. Because of the variation in soil strengths, site-specific shear strength data are required in order to perform an accurate slope stability analysis in the Mississippi Delta region of the Gulf of Mexico. For example, a factor of safety of 1.8 was calculated using shear strength data from a boring in South Pass 54, which is consistent with the pipeline and platform at that location remaining undamaged. However, pipelines and a platform were damaged by mudslides just over a mile away in South Pass 55. Conversely, Mississippi Canyon 20, a factor of safety of 0.85 was calculated from the available shear strength profile, which is

consistent with the reported slope failure at the nearby platform. However, the boring is actually about one-half mile away from the platform. It is possible that the soil shear strength profile at the location of the platform is different from the profile found from the boring data, and, thus, the actual factor of safety at the platform may have been somewhat higher or lower than 0.85. It is important to understand these limitations when using the results of this study.

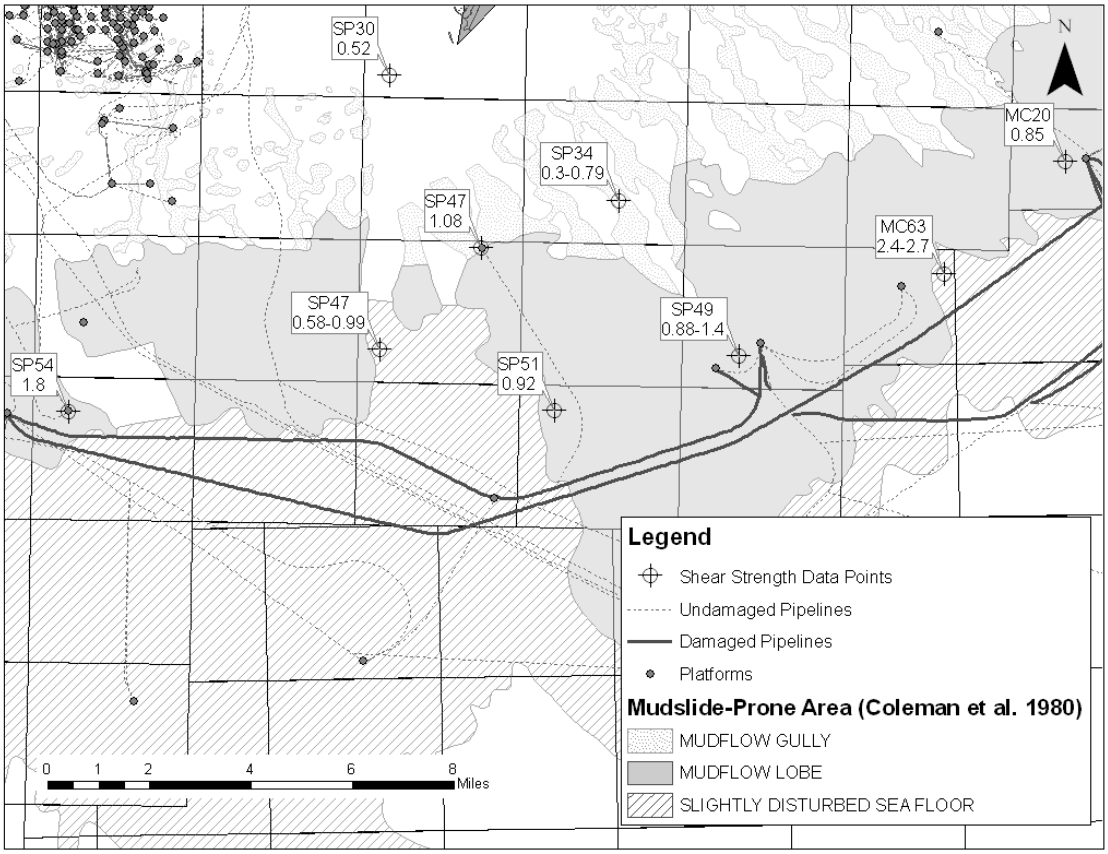

Figure 8. Overview of site-specific shear strength data points, illustrating the variability in factor of safety within lease blocks and between various geologic features

The only location in the Mississippi Delta region of the Gulf of Mexico where results of the limit equilibrium analysis conflicted with reported mudslide activity is at Main Pass 70. At this location, a factor of safety of 0.93 was calculated, but the platform and pipeline where the boring was located did not fail. However, a factor of safety of 0.93 is not sufficiently less than 1.0 to conclusively state that failure should occur. Furthermore, this location is in very shallow water (less than 50 feet deep), and shallow water wave

effects such as breaking and bottom friction may have been underestimated in the hindcast that resulted in a computed factor of safety less than 1.0.

Results calculated using the limit equilibrium model are generally consistent with the mudslide activity that was reported during Hurricane Ivan. More site-specific shear strength data are necessary, however, to further validate the model. Additional shear strength data is currently being obtained, and validation of the model will continue as more shear strength data becomes available.

Mississippi Canyon Block 20 Analysis

Mississippi Canyon Block 20 is an area where evidence of mudslides during Hurricane Ivan was reported and where site-specific shear strength data were available. This site is used as an example to illustrate the effects of various parameters in the limit equilibrium model on the factor of safety.

Calculations were performed using the limit equilibrium model with the maximum wave height corresponding to the hindcast value[18] reported for Mississippi Canyon 20, as well as for wave heights corresponding to plus and minus one standard deviation of the hindcast maximum wave height. The peak spectral wave period reported in the hindcast[18] was used for the calculations in all three cases. The slope angle was varied from 1 to 6 percent. The factor of safety is plotted versus slope angle on Figure 9. The slopes in the Mississippi Canyon 20 location have inclinations ranging up to as high as 5 percent in some areas, making them well within the range where failure would be expected, i.e., where the factor of safety is less than 1.0 (Fig. 9). From Figure 9 it can be seen that where the slope angles are relatively small, the factor of safety is very sensitive to small changes in the slope angle.

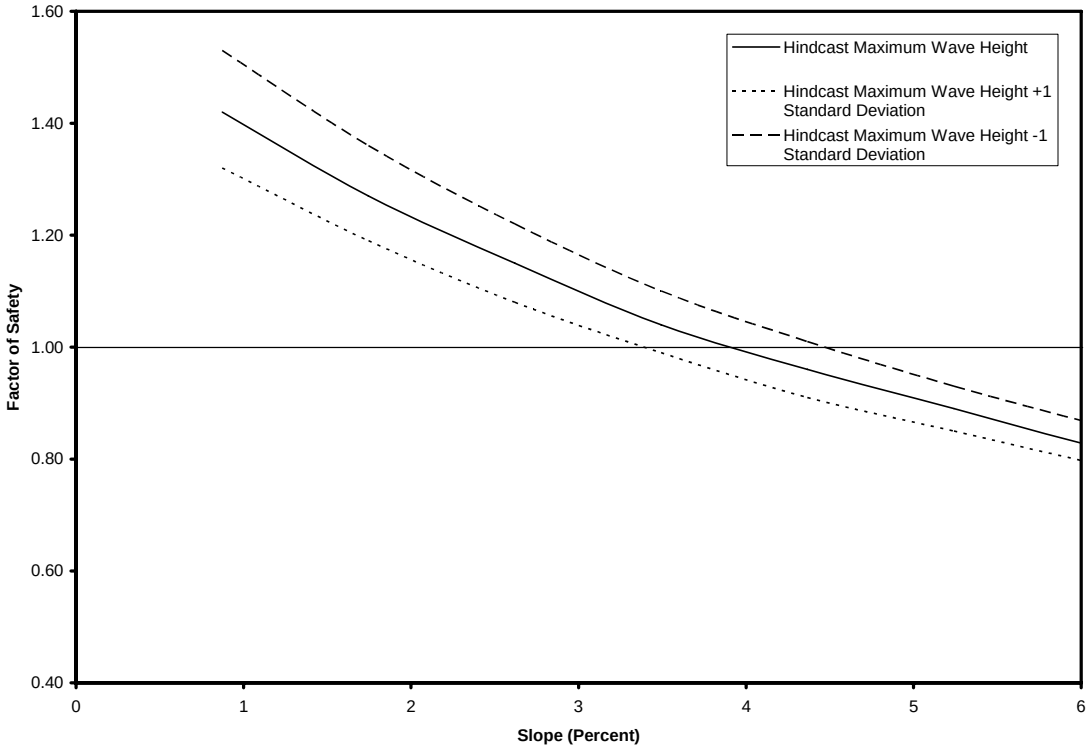

Figure 9. Effect of slope angle on factor of safety for Mississippi Canyon Block 20

These results indicate that the observed failure at Mississippi Canyon Block 20 is consistent both within a reasonable range for the slope angle and the wave loading. The results also indicate that slope inclinations of 3.5 percent or larger would have been susceptible to failure in this area.

One of the interesting aspects of Hurricane Ivan is that the wave periods were relatively long when compared with historic hurricanes. For example, Hurricane Camille in 1969 caused a mudslide in South Pass Block 70 (Bea et al.[2]). The peak spectral period during Hurricane Camille in South Pass Block 70 was 12.5 seconds. In contrast, the peak spectral period was 16.1 seconds during Hurricane Ivan in Mississippi Canyon 20. A longer wave period will produce greater bottom pressures in deeper water. The variation in factor of safety with water depth is shown in Figure 10 for wave periods of 12.5 and 16.1 seconds. The values shown are based on a seafloor slope of 3.5 percent, and a wave height of 71 feet, which is the hindcast wave height for the Mississippi Canyon 20 location. The 71-foot wave with a period of 12.5 seconds could produce instabilities

(factor of safety of 1.0 or less) in water depths up to 320 feet, while the longer period, 16.1-second wave could produce instabilities up to water depths of almost 540 feet. Therefore, the possibility of hurricanes with longer-period waves increases the risk of mudslides in deeper water depths than previously expected.

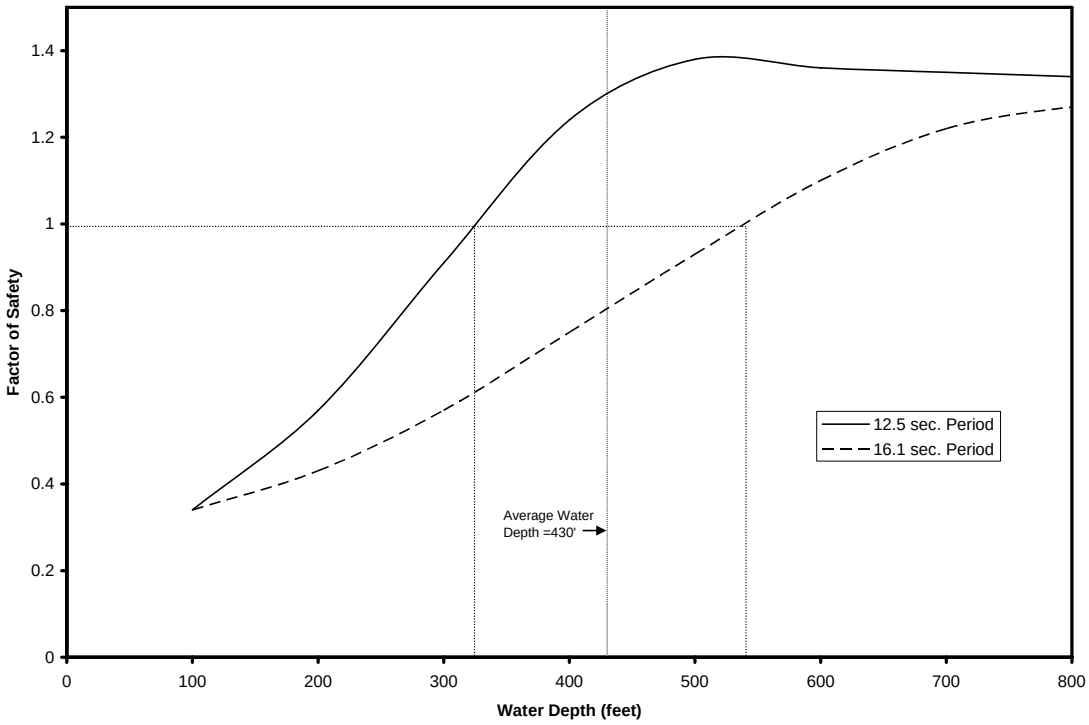

Figure 10. Effect of wave period on factor of safety at various water depths for Mississippi Canyon Block 20

STABILITY CHART FOR THE LIMIT EQUILIBRIUM MODEL

A chart has been developed that can be used to calculate the factor of safety against mudslide initiation for any location, assuming that the soil shear strength increases linearly with depth. The chart is shown in Figure 11. In order to use the chart, one must know the slope angle (β), water depth (d), wavelength (L), wave height (h), submerged unit weight of soil (γ'_s), unit weight of water (γ_w), the shear strength of the soil at the mudline (c_0), and the increase in shear strength with depth (c_z). The maximum pressure on the sea floor, p_{max}, is calculated using the following formula based on linear wave theory (Weigel[20]):

$$p_{\max} = \frac{\gamma_w}{2} \frac{h}{a\cos(2\pi \frac{d}{L})}.$$

This definition of p_{max} is an approximation of the pressures on the sea floor, but considering the uncertainties inherent in the evaluation of mudslide susceptibility, it is assumed to be a reasonable approximation. Future studies will examine the sensitivity of the results to the use of alternative wave theories to define p_{max}.

The factor of safety against mudslide initiation is calculated using the chart in Figure 11 and the following steps:

1. Calculate the maximum pressure on the sea floor, p_{max}, using the equation shown above.
2. Calculate the dimensionless constant: $\frac{\gamma' L \tan\beta}{p_{max}}$ using the known quantities.
3. Calculate the dimensionless constant: $\frac{c_z L}{c_0}$.

4. Using the values of $\frac{\gamma L \tan\beta}{p_{max}}$ and $\frac{c_z L}{c_0}$, calculated in steps 2 and 3 respectively, determine a value of $N_z = \frac{c_z L}{p_{\max} F}$ from Figure 11. If necessary, interpolate between lines for intermediate values of $\frac{c_z L}{c_0}$.

5. Calculate the factor of safety as $F = \frac{1}{N_z}\left(\frac{c_z L}{p_{\max}}\right)$ using N_z from the chart in Figure 11 and known values of c_z, L and p_{max}.

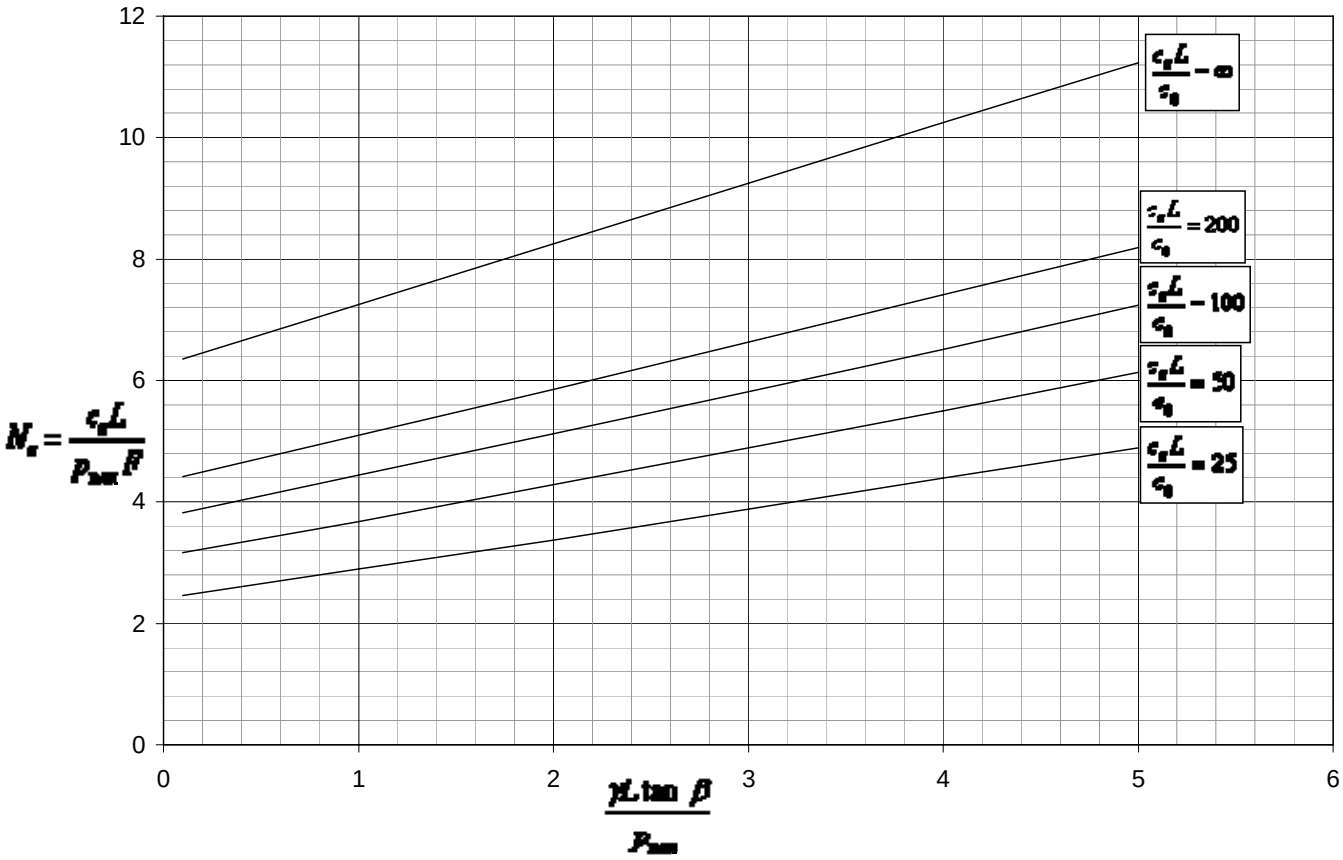

Figure 11. Chart to calculate factor of safety against mudslide initiation for a strength profile increasing linearly with depth.

Figure 11. Chart to calculate factor of safety against mudslide initiation for a strength profile increasing linearly with depth.

Shear strength profiles at South Pass Block 70 and Mississippi Canyon Block 63 and the linear strength profiles used to approximate them are shown in Figure 12. Sample chart calculations for these sites are shown in Table 1.

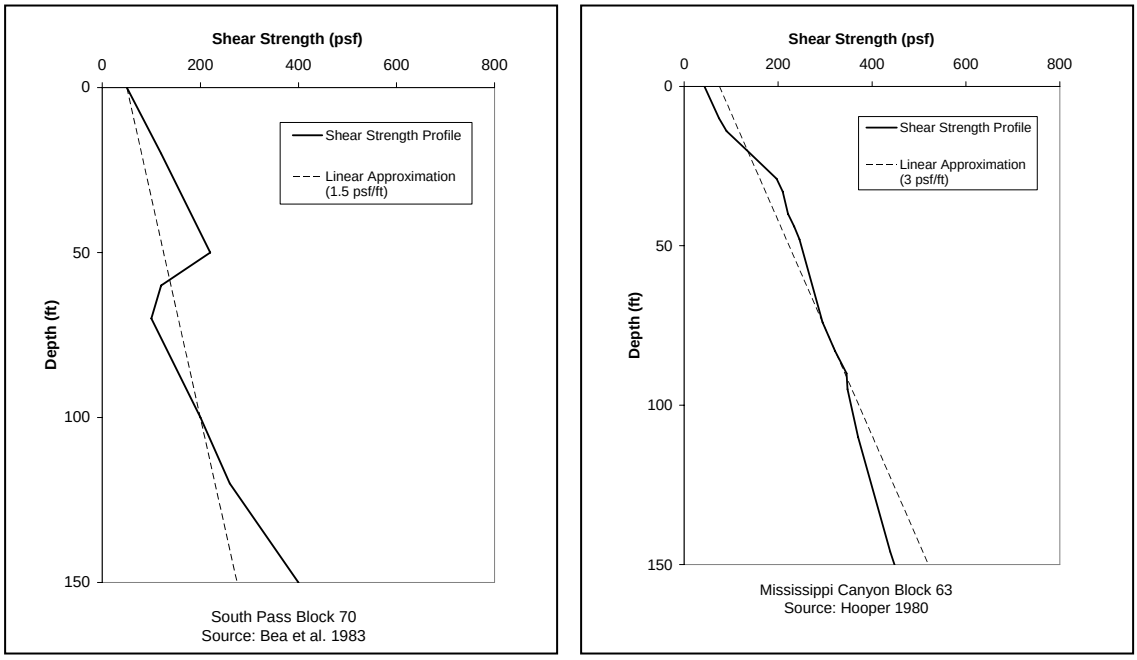

Figure 12. Shear strength profiles and corresponding linear strength profiles for example sites

Table 1. Sample factor of safety calculations using chart for linear increase in strength

Lease Block	Slope Angle (radians)	Water Depth (ft)	Wavelength (ft)	Wave Height (ft)	Submerged Soil Unit Wt. (pcf)	Water Unit Wt. (pcf)	P_{max} (psf)	$\frac{\gamma' L \tan\beta}{P_{max}}$
SP-70	0.0023	335	1341	73	30.0	64	931.91	0.1004
MC-63	0.0167	495	1260	69	30.0	64	371.42	1.6961

Lease Block	c_z (psf/ft)	c_0 (psf)	$\frac{c_z L}{c_0}$	N_z	F (from chart)	F (using actual shear strength profile)	Percent Difference (%)
SP-70	1.5	50	40.2	3.0	0.72	0.76	5.3
MC-63	3	75	50.4	4.1	2.48	2.43	2.1

The factors of safety calculated using the charts at these locations are within about 5% of those calculated using the limit equilibrium model with piecewise linear profiles. For locations with more variable strength profiles, the chart calculations are less accurate, because it is difficult to approximate these profiles by a simple linear increase in strength

with depth. Caution and conservatism should be used when approximating shear strength profiles with a linear increase in strength, because features such as high-strength crusts and other strength variations can significantly change the behavior of the soil. For sites with non-linear soil profiles, a linear profile representing a lower bound strength can safely be used as a first conservative estimate of the factor of safety. However, it is recommended that the limit equilibrium model with the full piecewise linear strength profile be used in cases where the strength profile is variable, as presented in the attached spreadsheet program and described in Appendix 3.

CONCLUSION

Results of this study suggest that the simple limit equilibrium model works well to predict the factor of safety against mudslide initiation for a given location, particularly if site-specific shear strength data are available. The model is well-suited to quantify the effects of wave height and period, water depth, slope angle, and profile of undrained shear strength versus depth for potential mudslides. The model also shows that a noteworthy feature of Hurricane Ivan is the relatively long wave periods, which probably produced mudslides in deeper water than a typical hurricane such as Hurricane Camille would.

This report presents two simple and practical methods of calculating the factor of safety against mudslide initiation using the limit equilibrium model. The attached spreadsheet program can be used if the soil profile is highly variable. If the soil profile has a nearly linear increase in strength, the chart shown in Figure 10 can be used to calculate the factor of safety. Both of these methods are relatively user-friendly and can be used to estimate the mudslide risk to future or existing platforms and pipelines.

The data currently available also suggest that all mudslides caused by Hurricane Ivan occurred in or very near to the mudslide-prone area delineated by Coleman et al.[2], and for the most part damage was restricted to the mud lobes within the mudslide-prone area.

The researchers continue to collect additional data to verify and extend the analyses presented in this report. As additional shear strength data and details on mudslide damage continue to become available, the findings of this research will be updated. Results will be reported in future publications and reports.

References

1. Sterling, G.H. and Strobeck, E.E. (1973), "The Failure of the South Pass 70 B Platform in Hurricane Camille," *Proc. Offshore Technology Conference*, Houston, Texas, OTC Paper No. 1898.

2. Coleman, J.M., Prior, D.B., and Garrison, L. (1980), *Minerals Management Service Open File Report 80-02*, Maps 1-8.

3. Minerals Management Service (2005), List of pipelines damaged in hurricane Ivan by lease block, MMS Gulf of Mexico Region.

4. Coyne, M.J., and Dollar, J.J. (2005), "Shell Pipeline's Response and Repairs after Hurricane Ivan," *Proc. Offshore Technology Conference*, Houston, Texas, OTC Paper No. 17734.

5. Thompson, J., Garrett, M., Taylor, M., and George, T. (2005), "Sonar surveys for pipeline inspection show extent of pipeline displacement and seafloor instability following Hurricane Ivan," *Proc. Offshore Technology Conference*, Houston, Texas, OTC Paper No. 17738.

6. Minerals Management Service (2006), Pipelines in Gulf of Mexico Region, ArcInfo EEO File 8219-148, 409, 677.

7. Henkel, D.J. (1970), "The Role of Waves in Causing Submarine Landslides," *Geotechnique*, Vol. 20, No. 1, pp. 75-80.

8. Wright, S.G. and Dunham, R.S. (1972), "Bottom Stability Under Wave Induced Loads," *Proc. Offshore Technology Conference*, Houston, Texas, OTC Paper No. 1603.

9. Wright, S.G. (1976), "Analyses for Wave Induced Sea-Floor Movements," *Proc, Offshore Technology Conference*, Houston, Texas, OTC Paper No. 2427B.

10. Schapery, R.A., and Dunlap, W.A. (1978), "Prediction of Storm-Induced Shear Bottom Movement and Platform Forces," *Proc. Offshore Technology Conference*, Houston, Texas, OTC Paper No. 3259.

11. Pabor, P.A. (1981), "Numerical Analyses of Wave-Induced Seafloor Movements," M. S./ Thesis, The University of Texas at Austin, May 1981.

12. Bea, R.G., Wright, S.G., Sircar, P., and Niedoroda, A.W. (1983), "Wave-Induced Slides in South Pass Block 70, Mississippi Delta region of the Gulf of Mexico," *Journal of Geotechnical Engineering*, Vol. 109, No. 4.

13. Dunlap, W., Holcombe, W., and Holcombe, T.(2004), *Shear Strength Maps of Shallow Sediments in the Gulf of Mexico*, OTRC Project Report, Library No. 09/04A126, Offshore Technology Research Center.

14. Hooper, J.R. (1996), "Foundation Soil Motion in South Pass 47," *Proc. Offshore Technology Conference*, Houston, Texas, OTC Paper No. 1898.

15. Hooper, J.R. (1980), "Crustal Layers in Mississippi Delta region of the Gulf of Mexico Mudflows." *Proc. Offshore Technology Conference*, Houston, Texas, OTC 3770.

16. Roberts, H.H., Cratsley, D.W., and Whelan, Thomas III (1976), "Stability of Mississippi Delta region of the Gulf of Mexico Sediments as Evaluated by Analysis of Structural Features in Sediment Borings," *Proc. Offshore Technology Conference*, Houston, Texas, OTC Paper No. 2425.

17. Quiros, G.W., Young, A.G. Pelletier, J.H., and Chan, J. H-C. (1983), "Shear Strength Interpretation for Gulf of Mexico Clays," *Proc. Conference on Geotechnical Practice in Offshore Engineering*, Austin, Texas.

18. Cox, A.T.,Cardone, V.J., Counillon, F., and Szabo, D. (2005), "Hindcast Study of Winds., Waves, and Currents in Northern Gulf of Mexico in Hurricane Ivan (2004)", *Proc. Offshore Technology Conference*, Houston, Texas, OTC Paper No. 17736.

19. Haring, R. E. and Heideman, J.W. (1978), "Gulf of Mexico Rare Wave Return Periods," *Proc. Offshore Technology Conference*, Houston, Texas, OTC Paper No. 3230.

20. Wiegel, R.L. (1964), *Oceanographical Engineering*, Prentice Hall, Inc., Englewood Cliffs, NJ.

APPENDIX A - EQUATIONS IN THE LIMIT EQUILIBRIUM MODEL

The equations comprising the limit equilibrium model used in this study are described in detail below.

Henkel's limit equilibrium model was used for the analyses presented in this paper. The geometry of the model is shown in Figure 1. The location of the potential slip circle is defined by its radius, R, and height, h, expressed as the perpendicular distance from the slope to the center of the circle. The center of the circle is assumed to lie as a line perpendicular to the slope at the "null" point where the induced wave pressures are zero.

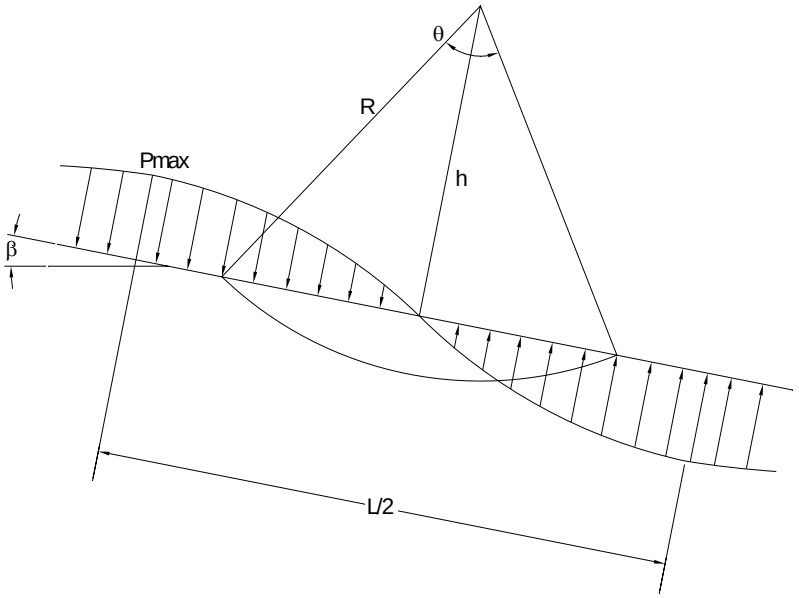

Figure A1. Geometry of the limit equilibrium model

A factor of safety is defined as the ratio of the developed shear stresses to the undrained shear strength of the soil, i.e.

$$F = \frac{c}{\tau} \qquad (1)$$

where "c" represents the undrained shear strength. The factor of safety in the following equations is calculated for a soil with a finite undrained strength at the ground surface and a linear increase in strength with depth. For cases where the undrained shear strength varied with depth, as it does for the actual strength profiles considered in this study,

piecewise linear variations in strength were assumed and integration was performed to calculate the resisting shear force. In the spreadsheet program included with this report, the factor of safety is calculated in this manner.

For the slope in Figure 1, the driving moment due to soil weight M_w is equal to:

$$M_w = W_s\, a \tag{2}$$

where W_S is the weight of soil and a is the moment arm of soil weight. The soil weight, W_s, is equal to:

$$W_s = \gamma'_s(\pi R^2\theta - h\sqrt{R^2 - h^2}) \tag{3}$$

where γ'_s is the submerged unit weight of the soil. The moment arm, a, is equal to:

$$a = \frac{2}{3} r \frac{\sin\left(\frac{\theta}{2}\right)^3}{\left(\frac{\theta}{2}\right) - \sin\left(\frac{\theta}{2}\right)\cos\left(\frac{\theta}{2}\right)} \sin\beta \tag{4}$$

The ocean wave induced pressures also contribute to the driving moment. The moment due to induced seafloor pressures is calculated as:

$$M_{wave} = 2p_{\max}\left[\left(\frac{L}{2\pi}\right)^2 \sin\left(\frac{2\pi X}{L}\right) - \frac{LX}{2\pi}\cos\left(\frac{2\pi X}{L}\right)\right] \tag{5}$$

where p_{max} is the maximum wave-induced pressure and L is the wavelength of the ocean wave. The length X is the chord length defined as:

$$X = R\sin\left(\frac{\theta}{2}\right) \tag{6}$$

Both the maximum wave pressure and the wavelength are calculated based on linear wave theory (Weigel[20]). The wavelength is calculated as:

$$L = \frac{gT^2}{2\pi}\tanh\frac{2\pi d}{L} \tag{7}$$

Where g is the acceleration of gravity, T is the wave period in seconds, and d is the water depth. The maximum wave pressure, p_{max} is equal to:

$$p_{\max} = \gamma_w \left(\frac{H}{\cosh\left(\frac{2\pi}{L} d \right)} \right) \tag{8}$$

Where H is the wave height and γ_w is the unit weight of sea water (Weigel[20]). In this analysis, it was assumed that the interaction of the waves with the sea floor was rigid.

The total driving moment is equal to:

$$M_d = M_w + M_{wave} \tag{9}$$

The resisting shear force is equal to:

$$S = \left(c_0 - K\gamma_s R \cos\left(\frac{\theta}{2} \right) \right) R\theta + 2K\gamma_s R^2 \sin\left(\frac{\theta}{2} \right) \tag{10}$$

where c_0 is the undrained strength at the ground surface (mudline) and z is the depth below the ground surface, measured perpendicular to the slope. K is equal to the rate of change in strength with effective stress $(ds_u/dz)/\gamma_s$, where s_u = undrained strength of soil. The resisting moment is equal to:

$$M_r = SR \tag{11}$$

A factor of safety can be calculated as the ratio of the resisting moment to the driving moment:

$$F = \frac{M_r}{M_d} \tag{12}$$

The factors of safety calculated based on Equation 12 are identical to those expressed earlier by Equation 1 in terms of the shear strength.

APPENDIX B – SHEAR STRENGTH PROFILES FROM PUBLIC SOURCES

All strength profiles used in this study are shown below with the exception of the profile in Mississippi Canyon Lease Block 20, which was obtained from a private source. The bold, solid lines represent shear strength data obtained from public boring logs. The bold, broken lines represent shear strength data interpreted from shear strength contour maps of the Gulf of Mexico, obtained from a proprietary source. The contour maps were created by a geotechnical consulting company for the purpose of offshore project planning. For the analyses in this study, the shear strength data obtained from the contour maps were used to complete those profiles that terminated at depths less than 150 feet. Profiles that were completed in this manner include South Pass 54, West Delta 107, Main Pass 70, Main Pass 77, and South Pass 30. The data obtained from the contour maps for depths of 60 feet to 150 feet are shown on all soil profiles for comparison, with the exception of Mississippi Canyon 63, as the contour maps did not include this location.

The lightweight, dotted lines represent linear shear strength profiles of 2 and 8 psf per foot. These linear profiles are shown for reference.

Data for all strength profiles was corrected with the modification factors used by Dunlap et al.[12]. These modification factors adjust strengths obtained from all testing methods to the reference strength of an unconfined compression test performed on a sample obtained using a 3-inch thin-walled sampler pushed into the soil.

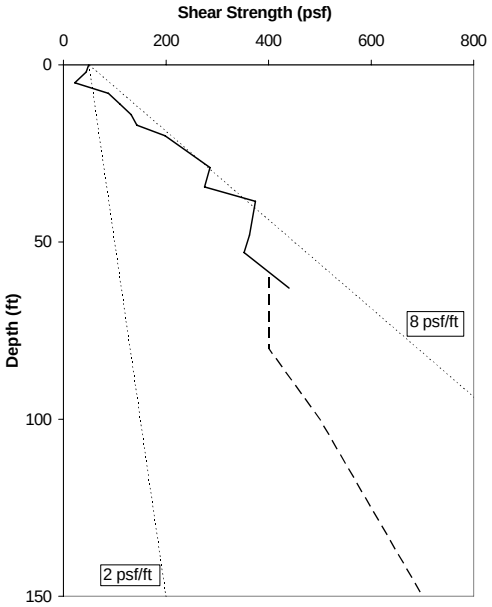

South Pass Block 54
Source: Final Project Report, MMS Project No. 367

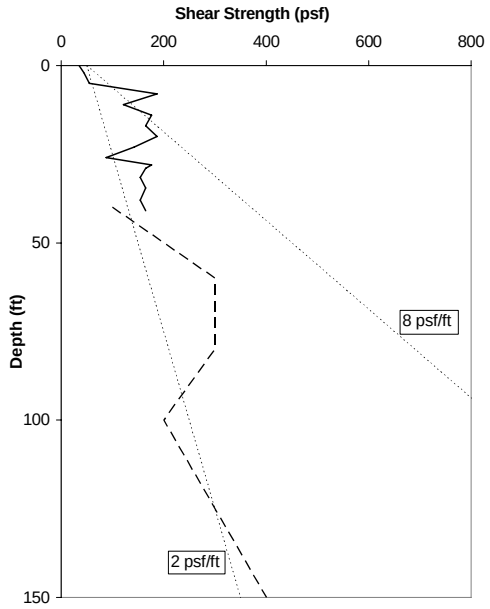

West Delta Block 107
Source: Final Project Report, MMS Project No. 367

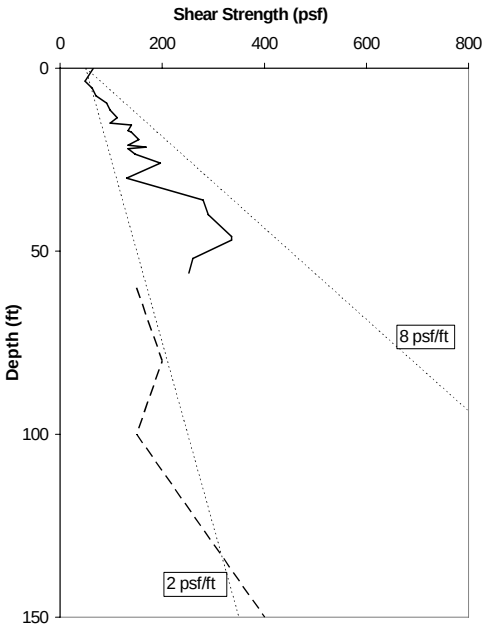

Main Pass Block 77
Source: Final Project Report, MMS Project No. 367

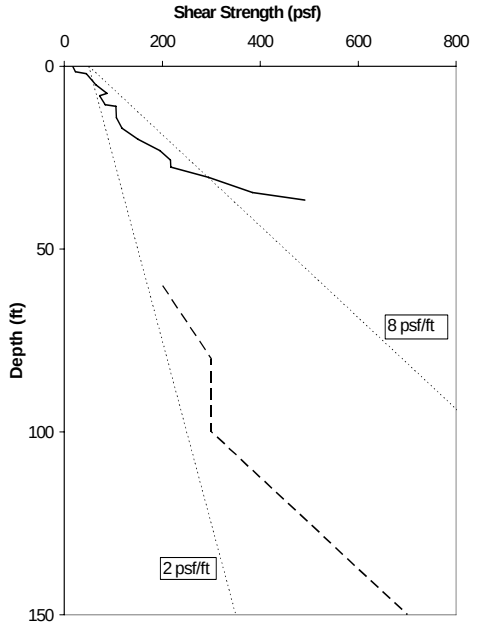

Main Pass Block 70
Source: Final Project Report, MMS Project No. 367

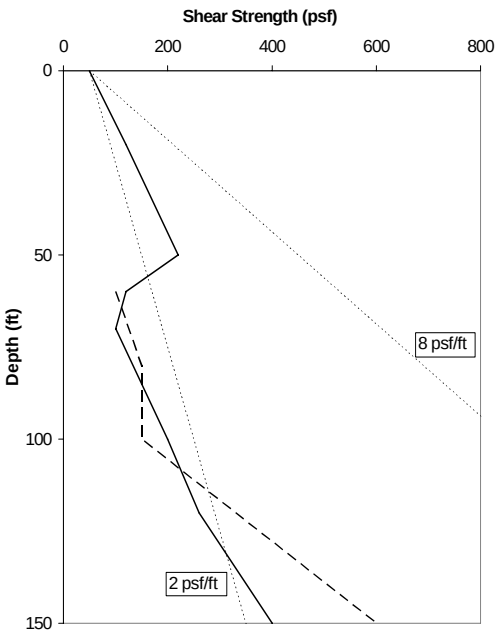

South Pass Block 70
Source: Bea et al. 1983

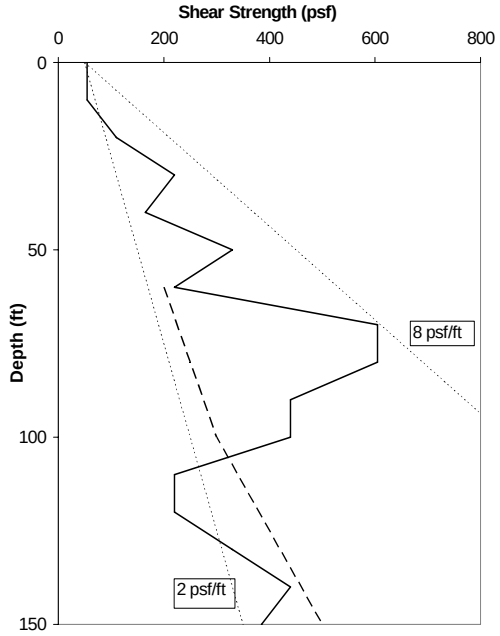

South Pass Block 47
Source: Hooper 1996

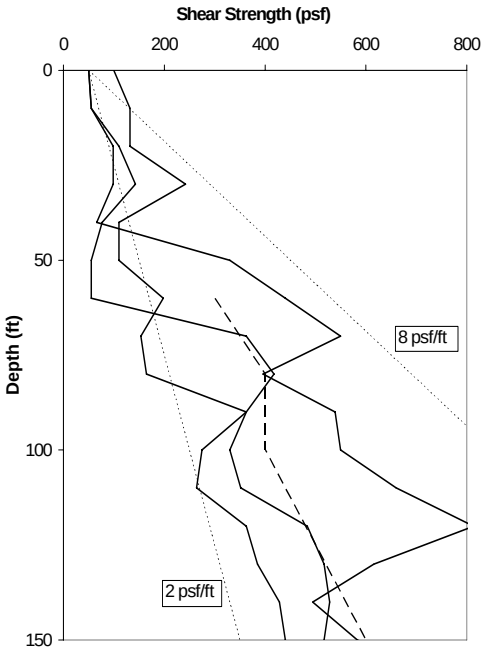

South Pass Block 47
Source: Roberts et al. 1976

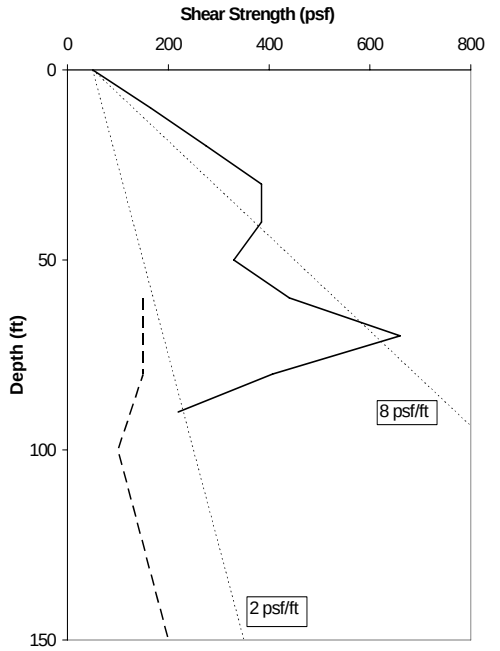

South Pass Block 30
Source: Roberts et al. 1976

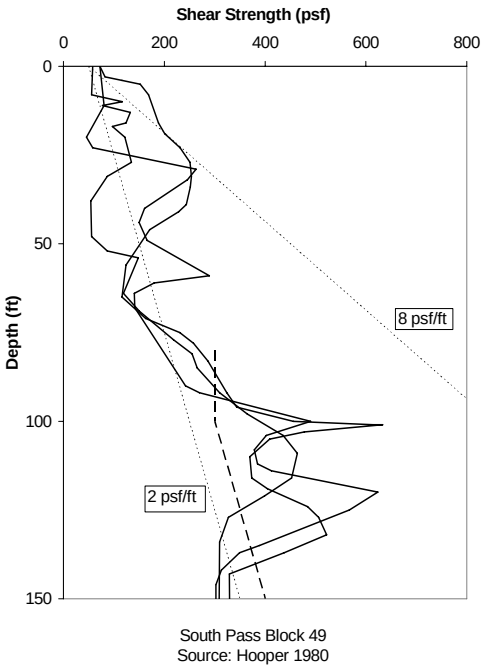

South Pass Block 49
Source: Hooper 1980

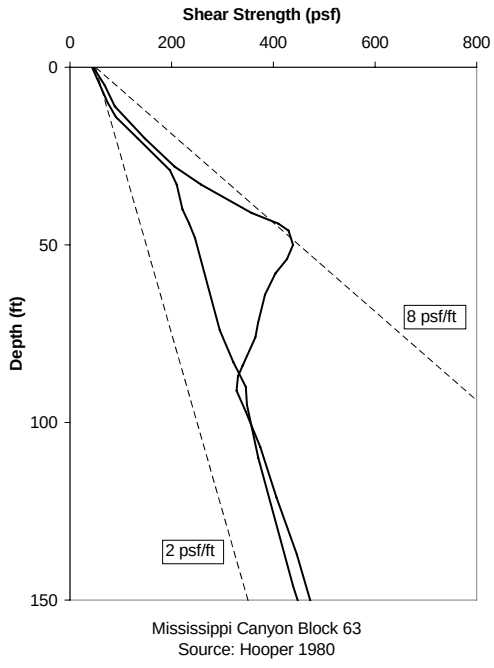

Mississippi Canyon Block 63
Source: Hooper 1980

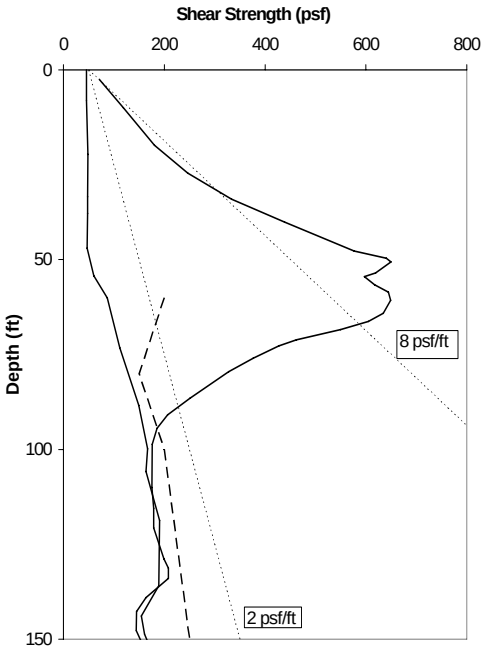

South Pass Block 34
Source: Hooper 1980

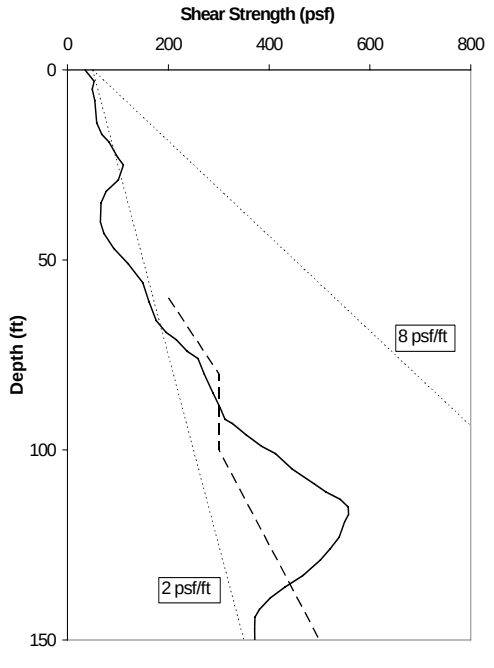

South Pass Block 51
Source: Hooper 1980

APPENDIX C - USER'S GUIDE FOR THE LIMIT EQUILIBRIUM SPREADSHEET PROGRAM

The spreadsheet program that was developed for this study is included with this report as a Microsoft Excel file. The spreadsheet program can be used to calculate a factor of safety against mudslide initiation for any site where the undrained shear strength varies in a piecewise linear pattern with depth.

The input parameters for the spreadsheet include:

- Slope angle (β)
- Water depth (d)
- Wavelength (L)
- Wave height (h)
- Submerged soil unit weight (γ'_s)
- Water unit weight (γ_w)
- Any soil shear strength profile with up to 50 data points
- A range of trial circle heights (h) – see Figure 1

Assumptions incorporated into the limit equilibrium model include:

- Slip surface is circular
- Soil unit weight, γ'_s, is constant
- The slope, β, is uniform
- Soil layers run parallel to the slope
- Bottom pressure, p_{max}, is calculated using linear wave theory (assumes a rigid sea floor)

The spreadsheet calculates the minimum factor of safety for a site by calculating the factors of safety for various slip circles. The size of the circle is dictated by its radius, R, and the height, h, of its center point above the slope, as shown in Figure 1.

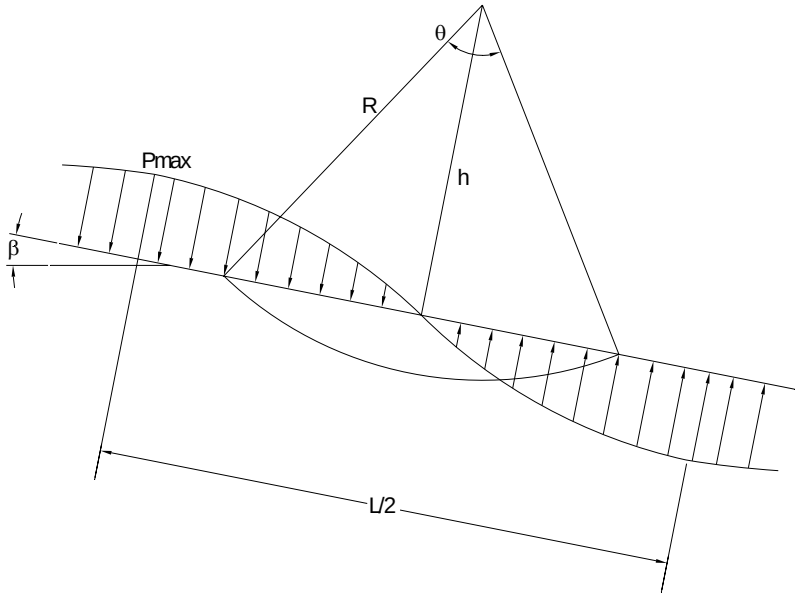

Figure C1. Model geometry

The user interface for the spreadsheet program is shown in Figure 2. For simplicity, the shear strength profile is defined by only six data points. The user can enter up to 50 data points to define the shear strength profile in the spreadsheet program.

Slope Angle (rad)	Water Depth (ft)	Wavelength (ft)	Wave Height (ft)	Submerged Soil Unit Wt. (pcf)	Water Unit Wt. (pcf)	Maximum Wave Pressure (psf)
β	d	L	H	γ'_s	γ_w	p_{max}
0.0100	**350**	**1000**	**70**	**30.0**	**64**	490.80

Minimum Factor of Safety = **0.80**

Trial Heights, h (ft)	Corresponding Factors of Safety
50	0.936
100	0.852
150	0.815
200	0.801
250	0.804
300	0.807
350	0.818
400	0.833
450	0.852
500	0.874
550	0.899

Shear Strength Profile

Critical height, h (ft)	Depth (ft)	Shear Strength (psf)	Radius of circle, r (ft)	Factor of Safety, F
200	**0**	**50**		
	50	**105**	**250**	**0.99**
	100	**139**	**300**	**0.81**
	150	**167**	**350**	**0.80**
	200	**175**	**400**	**0.82**
	250	**196**	**450**	**0.91**

Figure C2. User interface for the spreadsheet program

All cells requiring user input are highlighted blue in the spreadsheet program and are highlighted light gray in the figures contained in this Appendix. English units are listed for all values in the spreadsheet, but SI units can be used as long as units are consistent.

Steps to Using the Spreadsheet Program

1. *Initial input and calculated values*

Initial input values are typed into the spreadsheet in the cells shown circled in Figure 3. The contents of the various cells in which data are entered are described further below. The resulting values calculated in the spreadsheet program are also described. The equations used for all calculations are shown in Appendix 1.

Slope Angle (rad)	Water Depth (ft)	Wavelength (ft)	Wave Height (ft)	Submerged Soil Unit Wt. (pcf)	Water Unit Wt. (pcf)	Maximum Wave Pressure (psf)
β	d	L	H	γ'_s	γ_w	p_{max}
0.0100	350	1000	70	30.0	64	490.80

Minimum Factor of Safety = **0.80**

Trial Heights, h (ft)	Corresponding Factors of Safety
50	0.936
100	0.852
150	0.815
200	0.801
250	0.804
300	0.807
350	0.818
400	0.833
450	0.852
500	0.874
550	0.899

Shear Strength Profile

Critical height, h (ft)	Depth (ft)	Shear Strength (psf)	Radius of circle, r (ft)	Factor of Safety, F
0	0	50		
	50	105	50	2.38
	100	139	100	1.60
	150	167	150	1.32
	200	175	200	1.16
	250	196	250	1.10

Figure C3. Locations of initial input values

Site Parameters

The slope angle (in radians), water depth, wavelength, wave height, submerged unit weight of soil, and unit weight of water for the site are entered into the cells shown circled in Figure 4. The equation to calculate wavelength from wave period is presented in Appendix 1.

Slope Angle (rad)	Water Depth (ft)	Wavelength (ft)	Wave Height (ft)	Submerged Soil Unit Wt. (pcf)	Water Unit Wt. (pcf)	Maximum Wave Pressure (psf)
β	d	L	H	γ'_s	γ_w	p_{max}
0.0100	**350**	**1000**	**70**	**30.0**	**64**	490.80

Figure C4. Site parameters

The maximum pressure caused by the wave on the sea floor, shown circled in Figure 5, is calculated from the water depth, wavelength, wave height, and unit weight of water.

Slope Angle (rad)	Water Depth (ft)	Wavelength (ft)	Wave Height (ft)	Submerged Soil Unit Wt. (pcf)	Water Unit Wt. (pcf)	Maximum Wave Pressure (psf)
β	d	L	H	γ'_s	γ_w	p_{max}
0.0100	**350**	**1000**	**70**	**30.0**	**64**	490.80

Figure C5. Maximum pressure on the sea floor

Undrained Shear Strength Profile

The variation in undrained shear strength with depth is entered into the cells shown circled in Figure 6. Up to fifty points can be entered into the spreadsheet program to describe the shear strength profile.

Shear Strength Profile

Critical height, h (ft)	Depth (ft)	Shear Strength (psf)	Radius of circle, r (ft)	Factor of Safety, F
0	**0**	**50**		
	50	**105**	**50**	**2.38**
	100	**139**	**100**	**1.60**
	150	**167**	**150**	**1.32**
	200	**175**	**200**	**1.16**
	250	**196**	**250**	**1.10**

Figure C6. Shear strength profile

Trial Circle Heights

A number of trial heights for the centers of circles are entered into the cells shown circled in Figure 7. The factor of safety associated with each trial height will be calculated in the column to the right of the designated heights. The height of the critical circle (that with the lowest factor of safety) will be chosen from among the trial heights entered. For the Gulf of Mexico sites investigated, the critical circle height was typically between 200 and 500 feet. Accordingly, 50 to 100 feet is a good starting value for the heights. The factor of safety is not particularly sensitive to height. Thus, the increment between heights can be relatively large. Increments between 25 and 100 feet are sufficient. The example below uses a starting height of 50 feet, a maximum height of 550 feet, and increments of 50 feet. The critical factor of safety of 0.801 falls within the range of heights specified. Notice the small change in factor of safety (0.801-0.936) over the large range in height.

Trial Heights, h (ft)	Corresponding Factors of Safety
50	0.936
100	0.852
150	0.815
200	0.801
250	0.804
300	0.807
350	0.818
400	0.833
450	0.852
500	0.874
550	0.899

Figure C7. Trial heights

Once the initial input values have been entered, the minimum factor of safety is displayed in the upper right corner of the spreadsheet, in the cell shown circled in Figure 8.

Slope Angle (rad)	Water Depth (ft)	Wavelength (ft)	Wave Height (ft)	Submerged Soil Unit Wt. (pcf)	Water Unit Wt. (pcf)	Maximum Wave Pressure (psf)
β	d	L	H	γ'_s	γ_w	p_{max}
0.0100	**350**	**1000**	**70**	**30.0**	**64**	490.80

Minimum Factor of Safety = **0.80**

Trial Heights, h (ft)	Corresponding Factors of Safety
50	0.936
100	0.852
150	0.815
200	0.801
250	0.804
300	0.807
350	0.818
400	0.833
450	0.852
500	0.874
550	0.899

Shear Strength Profile

Critical height, h (ft)	Depth (ft)	Shear Strength (psf)	Radius of circle, r (ft)	Factor of Safety, F
0	**0**	**50**		
	50	**105**	**50**	**2.38**
	100	**139**	**100**	**1.60**
	150	**167**	**150**	**1.32**
	200	**175**	**200**	**1.16**
	250	**196**	**250**	**1.10**

Figure C8. Factor of safety calculated from initial input values

2. *Check that the factor of safety is a minimum*

To verify that the factor of safety calculated is a minimum factor of safety for the given set of input parameters, the minimum factor of safety must be located in the column labeled "Corresponding Factors of Safety," as shown in Figure 9. The column shows the factors of safety corresponding to each of the trial heights. The minimum factor of safety must lie somewhere within the range of heights designated as input.

Trial Heights, h (ft)	Corresponding Factors of Safety
50	0.936
100	0.852
150	0.815
200	0.801
250	0.804
300	0.807
350	0.818
400	0.833
450	0.852
500	0.874
550	0.899

Figure C9. Minimum factor of safety within range of heights

If the minimum factor of safety corresponds to either the maximum or the minimum trial height, the range of trial heights must be changed. For example, if the trial heights shown in Figure 9 began at 400 feet rather than at 50 feet, the range of heights and corresponding factors of safety would be as shown in Figure 10.

Trial Heights, h (ft)	Corresponding Factors of Safety
400	0.833
450	0.852
500	0.874
550	0.899
600	0.927
650	0.957
700	0.989
750	1.024
800	1.062
850	1.102
900	1.130

Figure C10. Minimum factor of corresponding with minimum height

The lowest factor of safety shown in this case would appear to be 0.833, while in reality the minimum factor of safety is 0.801. In order to ensure that the factor of safety calculated is a minimum, lower trial heights should be entered.

3. ***Selection of the critical circle and computation of its properties***

Once the height of the critical circle has been determined, the depth and radius of the circle can be calculated and the variation in factor of safety with circle depth can be examined. To compute the properties of the critical slip circle, the height corresponding to the minimum factor of safety must be typed into the box labeled "Critical Height," as shown in Figure 11.

Slope Angle (rad)	Water Depth (ft)	Wavelength (ft)	Wave Height (ft)	Submerged Soil Unit Wt. (pcf)	Water Unit Wt. (pcf)	Maximum Wave Pressure (psf)	Minimum Factor of Safety =
β	d	L	H	γ'_s	γ_w	p_{max}	**0.80**
0.0100	**350**	**1000**	**70**	**30.0**	**64**	490.80	

Trial Heights, h (ft)	Corresponding Factors of Safety
50	0.936
100	0.852
150	0.815
200	0.801
250	0.804
300	0.807
350	0.818
400	0.833
450	0.852
500	0.874
550	0.899

Shear Strength Profile

Critical height, h (ft)	Depth (ft)	Shear Strength (psf)	Radius of circle, r (ft)	Factor of Safety, F
200	**0**	**50**		
	50	**105**	**250**	**0.99**
	100	**139**	**300**	**0.81**
	150	**167**	**350**	**0.80**
	200	**175**	**400**	**0.82**
	250	**196**	**450**	**0.91**

Figure C11. Critical circle height entered in to table to calculate circle properties

Once the critical circle height has been entered, the radius for a circle corresponding to each depth in the shear strength profile is calculated by subtracting the depth from the circle height. The factors of safety for slip circles extending to each depth are calculated. The radii and factors of safety are shown circled in Figure 12.

Slope Angle (rad)	Water Depth (ft)	Wavelength (ft)	Wave Height (ft)	Submerged Soil Unit Wt. (pcf)	Water Unit Wt. (pcf)	Maximum Wave Pressure (psf)	Minimum Factor of Safety =
β	d	L	H	γ'_s	γ_w	p_{max}	**0.80**
0.0100	**350**	**1000**	**70**	**30.0**	**64**	490.80	

Trial Heights, h (ft)	Corresponding Factors of Safety
50	0.936
100	0.852
150	0.815
200	0.801
250	0.804
300	0.807
350	0.818
400	0.833
450	0.852
500	0.874
550	0.899

Shear Strength Profile

Critical height, h (ft)	Depth (ft)	Shear Strength (psf)	Radius of circle, r (ft)	Factor of Safety, F
200	**0**	**50**		
	50	**105**	**250**	**0.99**
	100	**139**	**300**	**0.81**
	150	**167**	**350**	**0.80**
	200	**175**	**400**	**0.82**
	250	**196**	**450**	**0.91**

Figure 12. Radii and factors of safety for slip circles extending to each depth in the shear strength profile

In order to find the properties of the critical slip circle, the value of the minimum factor of safety from the top of the spreadsheet must be located in the table of factors of safety shown circled in Figure 12. The corresponding radius and depth can then be found. In the example shown in Figure 13, the critical slip circle has a depth of 150 feet and a radius of 350 feet.

Slope Angle (rad)	Water Depth (ft)	Wavelength (ft)	Wave Height (ft)	Submerged Soil Unit Wt. (pcf)	Water Unit Wt. (pcf)	Maximum Wave Pressure (psf)
β	d	L	H	γ'_s	γ_w	p_{max}
0.0100	**350**	**1000**	**70**	**30.0**	**64**	490.80

Minimum Factor of Safety = **0.80**

Trial Heights, h (ft)	Corresponding Factors of Safety
50	0.936
100	0.852
150	0.815
200	0.801
250	0.804
300	0.807
350	0.818
400	0.833
450	0.852
500	0.874
550	0.899

Shear Strength Profile

Critical height, h (ft)	Depth (ft)	Shear Strength (psf)	Radius of circle, r (ft)	Factor of Safety, F
200	**0**	**50**		
	50	**105**	**250**	**0.99**
	100	**139**	**300**	**0.81**
	150	**167**	**350**	**0.80**
	200	**175**	**400**	**0.82**
	250	**196**	**450**	**0.91**

Figure C13. Identification of properties of the critical slip circle